Leveraging Neutrosophic TOPSIS with Artificial Intelligence-Driven Tropical Cyclone Intensity Estimation for Weather Prediction

Fuad S. Al-Duais[1], Shoraim M. H. A[2], Amal O. A. Al magdashi[3], Badr Eldeen A. A. Abouzeed[4]

[1]Department of Mathematics, College of Science and Humanities in Al-Kharj, Prince Sattam Bin Abdulaziz University, Al-Kharj 11942, Saudi Arabia
[2]Department of Economics and Policy Sciences, College of Commerce and Economics, Hodeida University, Hodeida, Yemen.
[3]Department of Marketing and Production. Faculty of Administrative Sciences Thamar University, Yemen.
[4]Department of Economics, Faculty of Economics and Commercial, University of kordofan, sudan
Emails: F.alduais@psau.edu.sa; majedsh107@gmail.com; Amal.almaqdashi@tu.edu.ye; badralhaj2014@gmail.com

Abstract

Tropical cyclones (TCs) are powerful, low-pressure weather systems attributed to heavy rainfall and strong winds, and have often resulted in extensive damage to coastal regions. TC intensity prediction, an essential aspect of meteorological forecasting, includes evaluating the strength of the storm to facilitate disaster preparedness and alleviate possible risks. Classical approaches for the prediction of TC intensity rely on different oceanic and atmospheric parameters, but the incorporation of artificial intelligence (AI) approaches, especially those leveraging image data, provides positive breakthroughs in efficiency and accuracy. By harnessing AI techniques like deep learning architectures and convolutional neural networks (CNNs), meteorologists could analyze radar data, satellite imagery, and other visual inputs to distinguish complicated patterns indicative of intensity changes and TC development. This combination of weather science and AI-driven image analysis enables more timely and precise predictions and improves our understanding of TC dynamics, eventually fortifying protection against the impacts of formidable storms. This article introduces Neutrosophic TOPSIS with Artificial Intelligence Driven Tropical Cyclone Intensity Estimation (NTOPSIS-TCIE) technique for Weather Prediction. The presented NTOPSIS-TCIE technique determines the intensities of the TC which in turn helps to forecast weather. In the NTOPSIS-TCIE technique, median filtering (MF) approach is used to remove the noise in the images. In addition, the features are extracted using deep convolutional neural network (CNN) model. To enhance the performance of the CNN model, Harris Hawks Optimization (HHO) algorithm is applied. Finally, the NTOPSIS model is employed for the prediction of TC intensities. The performance of the NTOPSIS-TCIE technique can be studied using TC image dataset and the results signify its promising results over other models

Keywords: Tropical Cyclone; Artificial Intelligence; Neutrosophic; Weather Prediction; Harris Hawks Optimization

1. Introduction

Tropical cyclone (TC) is a dangerous climate action which contains most major effects on life of humans and assets and can affect disasters like dangerous winds and huge waves [1]. The positions of TC lifetime maximum intensities (LMI) are currently moving poleward, corresponding to the growth of the tropical zones affected by global warming. Therefore, LMI positions are transferring near coastlines by 30 kilometres per year, mainly in the Western North Pacific area [2]. Few studies recommend that the complete intensity of TC will upsurge, with slower fading of land-falling TCs owing to the enlarged atmospheric-soaked water vapor in the hotter climate [3]. The

Doi: https://doi.org/10.54216/IJNS.240209
Received: December 25, 2023 Revised: February 09, 2024 Accepted: April 21, 2024

socio and economic damage initiated by TCs in sea regions is only probable to enlarge in future, which recommends the significance of enhancing the capabilities of groups to estimate the positions and TCs intensity.

TC intensity is a significant feature in forecasting TC, and precise intensity prediction has significant economic and social importance [4]. The atmospheric method is an extremely non-linear chaotic model, and the initial value trouble and the mistake of the method might transport uncertainty. So, it is very essential to illustrate this uncertainty, affecting single-value to probabilistic predictions, thus enabling more complete decision-making and danger valuation [5]. While many research works were led on the forecast of TC intensity for past years, some development was created in the intensity performance forecast, which is a block in the area of meteorological predicting [6]. While some research work has tried to measure probabilistic predictions or TC's uncertainty equated with the concentration on deterministic predicting models. Presently, the probabilistic predicting of TC mostly implements the statistical and ensemble model [7].

Artificial intelligence (AI) models have currently prepared important developments in demonstrating and predicting in the earth sciences [8]. Also, AI has created major development in TC predicting, and the longer-term prediction of cyclone tracks has exceeded the act of prediction centers [9]. With the growth of ML models, particularly the arrival of neural networks by the activation function, numerous innovative techniques are used to estimate TC. The authors used Artificial Neural Networks (ANN) to increase the performance of non-linear autoregressive methods which predict cyclone conflicts [10]. Also, deep learning (DL) methods like employing a Convolutional Neural Network (CNN) that was intended to procedure imageries completely, were generally functional to acquire features from the satellite image data.

Zhao et al. [11] designed a multi-task learning algorithm called Multi-Task Graph Residual Network (MT-GN) to estimate and categorize the TC intensity from the FY-4A geostationary meteorological satellite image. New benchmark data was gathered from the FY-4A satellites for the intensity estimation and TC classification tasks. In our dataset, four dissimilar methods to the intensity estimate of TCs and classify TCs are compared. We found that accurate estimation and classification of TCs are accomplished, which needs co-related knowledge from all the processes. Therefore, a convolutional feature extractor was trained in a multi-task way. Moreover, a task-dependency embedding model is constructed by utilizing GCN that achieves better results. Kim et al. [12] introduce a CNN model for 24-hour predictions of the TC intensity changes and quick intensification over the western Pacific. The DeepTC is trained by means of amplitude focal loss, for capturing larger intensity changes, and rapid intensification (RI) events.

In [13], a TC intensity estimation technique using satellite images using the Xception architecture as a backbone. The key concept is to estimate the highest wind speed of TC through the image feature extractor. Firstly, the Laplacian pyramid image fusion technique for the water vapour (WV) and infrared (IR) channels of satellite images has been used to improve the overall quantity of input data. Next, an optimization technique for the width and depth of the Xception architecture is introduced to improve the estimation accuracy and reduce the parameter redundancy. Moreover, a dual attention module focuses on the important region of cyclone images. Kumar et al. [14] developed a TC intensity prediction LSTM with CSO. The LSTM technique is enhanced through CSO method for reducing the prediction errors and improving accuracy.

Tian et al. [15] developed a dynamic balance CNN to resolve these challenges. The model has two different branches, the former is learning of raw information, and the latter is the learning of strong (weak) TCs. The model is adjusted dynamically by the tradeoff parameter from the learning of raw information to the strong (weak) TCs, thereby decreasing errors in underestimation of strong (weak) TCs. In [16], proposed a new DL-based TC intensity prediction network called Pre_3D that extracts inter- and intra-feature of TC intensity. An MLP network achieves versatile combination of the two features for correct estimate of TC intensity. In [17], proposed a new TC intensity estimation technique for the TC intensity estimate from the multi-spectral infrared images. The deep multisource attention network (DMANet) is introduced to design the dynamics of the spatial dimension and multispectral infrared images.

This article introduces Neutrosophic TOPSIS with Artificial Intelligence Driven Tropical Cyclone Intensity Estimation (NTOPSIS-TCIE) technique for Weather Prediction. The presented NTOPSIS-TCIE technique determines the intensities of the TC which in turn helps to forecast weather. In the NTOPSIS-TCIE technique, median filtering (MF) approach is used to remove the noise in the images. In addition, the features are extracted using deep convolutional neural network (CNN) model. To enhance the performance of the CNN model, Harris Hawks Optimization (HHO) algorithm is applied. Lastly, the NTOPSIS approach was deployed for the prediction of TC intensities. The performance of the NTOPSIS-TCIE technique can be studied using TC image dataset and the results signify its promising results over other models.

Doi: https://doi.org/10.54216/IJNS.240209
Received: December 25, 2023 Revised: February 09, 2024 Accepted: April 21, 2024

2. Background Information

Definition 1: Consider X as a space of objects (points) with typical components in X characterized by x [18]. The single-valued neutrosophic set (SVNS) A in X is represented as truth membership function (MF) $T_A(x)$, indeterminacy MF $I_A(x)$, and falsity MF $F_A(x)$. Following, an SVNS A is characterized as $A = \{x, T_A(x), I_A(x), F_A(x)x \in X\}$, where $T_A(x), I_A(x), F_A(x) \in [0,1]$ for all the points x in X. Thus, the sum of $T_A(x), I_A(x)$ and F_A

(x) fulfils the conditions $0 \leq T_A(x) + I_A(x) + F_A(x) \leq 3$. The SVN number is represented as $= (a\ b\ c)$, where $a, b, c \in [O, 1]$ and $a + b + c \leq 3$.

Definition 2: Consider $A_1 = (a_1, b_1, c_1)$ and $A_2 = (a_2, b_2, c_2)$ as SVN numbers, then sum between $A_1\ y\ A_2$ is described by:

$$A_1 + A_2 = (a_1 + a_2\text{-}\, a_1a_2, b_1b_2, c_1c_2) \tag{1}$$

Definition 3: Consider $A_1 = (a_1, b_1, c_1)$ and $A_2 = (a_2, b_2, c_2)$ as SVN numbers, then multiplication between A_1yA_2 is described by:

$$A_1 * A_2 = (a1a2, b1 + b2 - b1b2, c1 + c2 - c1c2) \tag{2}$$

Definition 4: Consider $A = (a, b, c)$ as a SVN number and $\lambda \in \mathbb{R}$ an random integer:

$$\lambda A = (1 - (1 - a)^{\lambda}, b^{\lambda}, c^{\lambda}), \lambda > 0 \tag{3}$$

Definition 5: Consider $A =* A_{1t}A_{22}\ tA_n +$ as a SVN numbers, whereas $Aj = (aj, bj, cj)j = 1,2, \dots, n)$ is defined by

$$\sum_{j=1}^{n} \lambda_j A_j = \left(1 - \prod_{j=1}^{n}(1 - a_j)^{\lambda_j}, \prod_{j=1}^{n} b_j^{\lambda_j}, \prod_{j=1}^{n} c_j^{\lambda_j}\right) \tag{4}$$

In Eq. (4), λ_j refers to the weighted of $A_j(j = 1,2, \dots, n)$, $\lambda_j \in [0,1]$ and $\sum_{j=1}^{n} \lambda_j = 1$

Definition 6. Consider $A^* = \{A_1^*, A_2^*, \dots, A_n^*\}$ as a set of n SVN numbers, $*= (aj *, bj *, cj *)$ $(j = 1,2, \dots, n)$, and $B_i = \{B_{i1}, B_{i2}, \dots, B_{im}\}(i = 1,2, \dots, m)$, $(j = 1,2, \dots, n)$ is given below:

$$s_i = (\frac{1}{3}\sum_{j=1}^{n}(|a_{ij} - a_j^*|)^2 + (|b_{ij} - b_j^*|)^2 + (|c_{ij} - c_j^*|)^2)^{\frac{1}{2}}(i = 1,2, \dots, m) \tag{5}$$

Definition 7: Consider $A = (a, b, c)$ as an SVN number, a score function S of SVN value, according to the truth-, indeterminacy-, and falsehood membership degree are given as:

$$S(A) = \frac{1 + a - 2b - c}{2} \tag{6}$$

Where $S(A) \in [-1,1]$

The score function S is decreased to the score function if $b = 0$ and $a + b \leq 1$.

A linguistic variable is considered as sentences or words rather than numbers in artificial or natural language and is formulated by the component of its term set. It is used to resolve decision-making problems. k-decision-maker evaluates the importance of m-alternative under n conditions and ranks the performance regarding linguistic statement transformed into SVN number. The decision-maker often uses a group of weights and the importance weight is based on SVN value of the linguistic term.

3. Materials and Methods

In this article, we have presented a novel NTOPSIS-TCIE algorithm for weather prediction. The presented NTOPSIS-TCIE technique determines the intensities of the TC which in turn helps to forecast weather. It contains distinct kinds of processes involved as MF-based preprocessing, CNN-based feature extractor, HHO-based parameter tuning, and NTOPSIS-based TC prediction. Fig. 1 defines the working flow of NTOPSIS-TCIE technique.

Doi: https://doi.org/10.54216/IJNS.240209
Received: December 25, 2023 Revised: February 09, 2024 Accepted: April 21, 2024

A. Image Preprocessing

At primary stage, the NTOPSIS-TCIE technique takes place MF approach is used to remove the noise in the images. MF is paramount in image processing for edge preservation and noise reduction [19]. Different from linear filters that calculate the weighted average of adjacent pixels, MF replaces all the pixel values within its neighborhood median values. This technique suppresses the sudden intensity changes or outliers, making it especially useful to remove salt-and-pepper noise while retaining image details.

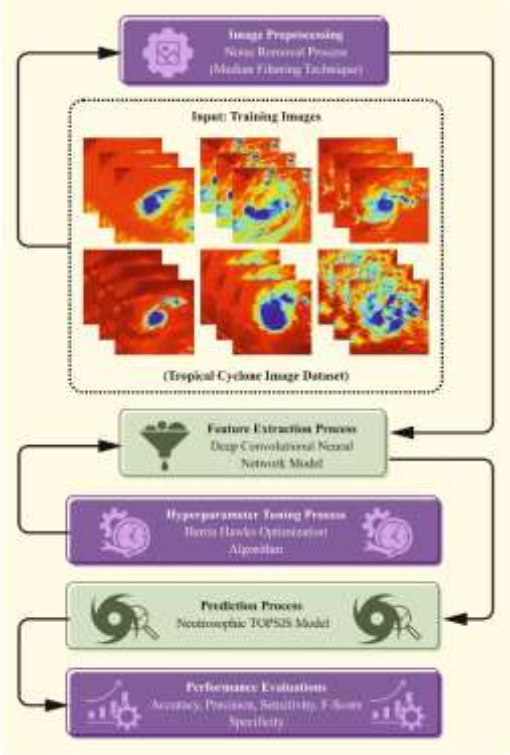

Figure 1: Workflow of NTOPSIS-TCIE technique

By considering local pixel value instead of intensities alone, MF generates smoother outcomes without blurring edges, which makes it a powerful tool for optimizing image quality in several applications, such as digital photography, medical imaging, and computer vision.

B. Feature Extractor

In addition, the features are extracted using deep CNN model. There are many varieties of artificial neural networks (ANNs), comprising CNNs [20]. CNNs are proficient in automatic learnable hierarchies of features in input image matrices instead of handcrafted features mined by intricate techniques. Recently, the CNN methods have accomplished numerous revolutionary developments in CV that comprise object tracking, segmentation, and classification. Due to some connections and parameters, CNN model can have the ability to share and pool the weight factors. A standard CNN model contains various convolution layers embedded in each other accompanied by the FC layer. Fig. 2 demonstrates the infrastructure of CNN.

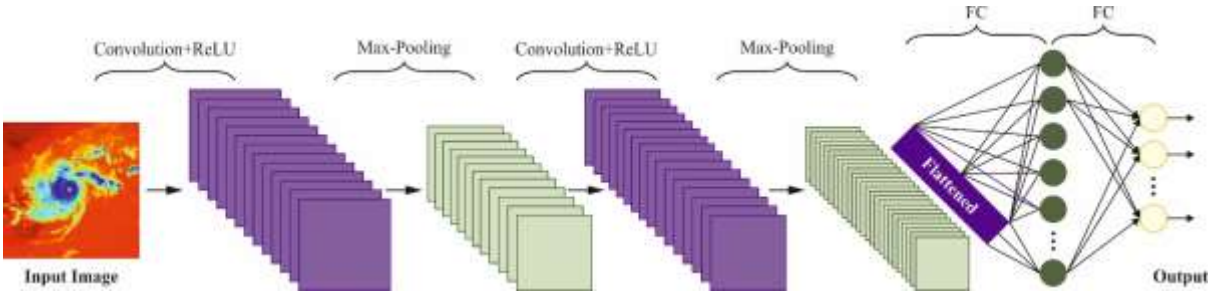

Figure 2: Structure of CNN Model

Doi: https://doi.org/10.54216/IJNS.240209
Received: December 25, 2023 Revised: February 09, 2024 Accepted: April 21, 2024

Input: The input of a CNN normally includes matrices of 1-channel gray images or 3-channel colour that have intensity values at every location.

Convolution (Conv) layer: The output of final layer must be filtered in the smaller area through every Conv layer. Additionally, the filters have been typically smaller learnable matrices with dimensions 3x3 or 5x5. By employing parameter distribution, single filter has convolved through every spatial dimension for extracting a feature from an image.

ReLU: In Conv layer and FCL, ReLUs were generally utilized as an activation function for presenting nonlinear conversion. The mathematical equation for this function will be represented as $f(x) = \max(0, x)$. This can be proved by experimentation in which ReLU becomes greater than standard sigmoid function in the expansion of deep network and it avoids gradient saturation and training convergence when preserving as many possible new values.

Pool: It has potential to decrease the spatial dimension of the output via down sampling the spatial dimension in a nonlinear way through the pooling layer. To decrease the computational rates and network parameters, it is essential to decrease its parameters. The input feature map has been positioned amongst two following Conv layers.

FCL: The FCLs have been the boundary of an ANN. During final layer, there is a connection among all the neurons in the FCL. Several N neurons at the final FCL of such a network can produce the output by employing each input label. The probability of performance to every label in the N-dimensional output will be computed through the softmax function.

$$P(z_i) = \frac{\exp(z_i)}{\sum_{i=1}^{N} \exp(z_i)} \tag{7}$$

During 2nd final layer, $P(Z)$ signifies the probability of forecasting the i^{th} value. For making decisions, every layer should be stacked together to make a CNN.

C. Hyperparameter Tuning Process

At this stage, the hyperparameter tuning process of CNN model was executed by use of HHO. The HHO is a population-based model which connects the cooperative behavior displayed by Harris' hawks group, together with their separate searching approaches like establishing blockades, hunting prey, and implementing dives [21]. The system functions with dual main stages such as exploration, where latent victim is recognized, and exploitation contains direct attack, with obstructs and dives. This HHO algorithm contains numerous stages. At first, it evaluates the hawk's population vector and computes their value of fitness, besides classifying the finest location vector for prey. Then, it continues to adjust the resistance strength (J) and early energy (E) of prey, besides regulating its escaping energy at each iteration. These upgrades were performed utilizing Eqs (8)-(10). This technique permits the algorithm to dynamically adjust and improve its strategies to enhance the searching procedure for enhanced performance.

$$E_0 = 2rand() - 1 \tag{8}$$

$$J = 2(1 — ramd()) \tag{9}$$

$$E = 2E_0\left(1 - \frac{t}{t_{\max}}\right) \tag{10}$$

The stage of exploration is considered by attaining a prey escape energy value if the value is larger than 1. In this stage, the hawk location vector is repeatedly upgraded utilizing Eq. (10) to define its obstruct location. LB and UB represent lower and upper boundaries that demonstrate the finest position and minimum fit hawk in iteration t. $Xm(t)$ indicates the average population. In the stage of exploitation, 4 methods are famous:

Soft blockade: if prey's escape energy exceeds 0.5, then its effective escaping possibility is under 0.5. So the prey tries deceptive escaping, but the hawk tries the trick and finally searches it down over several blockades and actions.

Hard blockade (restricted energy): If both the parameters drop under 0.5, then it represents the lack of energy.

Soft blockade: The escape energy and ineffective escape exceeds 0.5. The prey tyres owing to consecutive hawk blockades, then finally fall upon prey to an amazing dive.

Doi: https://doi.org/10.54216/IJNS.240209
Received: December 25, 2023 Revised: February 09, 2024 Accepted: April 21, 2024

Hard blockade: If prey escapes energy is lesser than 0.5, then its ineffective escape chance is enhanced. So the prey's energy reduces and hawk hunts it unrestrained, including a surprise dive.

The algorithm further upgrades the hawk's location vector utilizing Eqs. (11) to (13). The algorithm completes after many iterations, with the fittest hawk effectively seizing the prey, representing the termination.

$$\vec{X}(t+1) = \Delta\vec{X}(t) - E\left|IV_{prey}(t) - \vec{X}(t)\right|, \Delta\vec{X}(t) \tag{11}$$

$$= \vec{X}_{\text{pery}}(t) - \vec{X}_{\text{pery}}(t) \tag{12}$$

$$\vec{X}(t+1) = \vec{X}_{\text{pery}}(t) - E\left|\Delta\vec{X}(t)\right| \tag{13}$$

$$\vec{X}(t+1) = \begin{cases} Y, F(Y) < F\big(X(t)\big) \\ Z, F(Z) < F\big(X(t)\big) \end{cases} \tag{14}$$

The HHO model is best in feature selection (FS) when compared to other models. It specifies that HHO proficiently classifies and positions the most relevant features from the database. It can produce the optimum feature subsets and underlines its efficiency in identifying features that expressively donate to the study's objects, possibly foremost to improve the performance of model.

The fitness choice is the key factor affecting the performance of the HHO technique. The hyperparameter selection method includes the solution encoded process to measure the efficiency of the candidate results. Here, the HHO approach considers accuracy as a key criterion to develop the FF that is expressed by.

$$Fitness \ = \ \max(P) \tag{15}$$

$$P = \frac{TP}{TP + FP} \tag{16}$$

Where TP and FP are the true and false positive values.

D. TC Prediction using NTOPSIS

Lastly, the NTOPSIS approach can be deployed for the prediction of TC intensities. The TOPSIS for SVNS used has the following: Assume $A = \{\rho_1, \rho_2, \dots \rho_m\}$ as a group of alternatives and $G = \{\beta_1, \beta_2, \dots, \beta_n\}$ as a set of criteria and the steps are given below:

Step 1: Define the relative importance of the experts: The specialist evaluates based on the linguistic scale, and the calculation is made with the related SVNN, consider $A_t = (a_t, b_t, c_t)$ the SVNS in line with t^{th} decision-makers $(t = 1,2, \dots, k)$.

$$\delta_\tau = \frac{a_t + b_t\left(\frac{a_t}{a_t + c_t}\right)}{\Sigma_{t=1}^{k} a_t + b_t\left(\frac{a_t}{a_t + c_t}\right)} \tag{17}$$

$\delta_t \geq 0$ and $\sum_{t=1}^{k} \delta_t = 1$

Step 2: Create neutrosophic decision matrix of aggregated unique value: This is represented as $D = \sum_{t=1}^{k} \lambda_t D^t$, where $d_{ij} = (u_{ij}, r_{ij}, v_{ij})$ aggregate each evaluation. d_{ij} refers to the aggregation of evaluation given by the experts $(u_{ij}^t, r_{ij}^t, v_{ij}^t)$. The matrix $D = (d_{ij})_{ij}$ is attained, where d_{ij} is a SVNN $(i = 1,2, m; j = 1,2, \dots, n)$.

Step 3: Define the Weight: Consider that the weight of all the criteria is represented as $W = (w_1, w_2, \dots, w_n)$, where w_j indicate the relative significance of criterion $\lambda_t w_j^t = (a_j^t, b_j^t, c_j^t)$. If it is the calculation of λ_t criteria by the t^{th} experts.

Step 4: Construct neutrosophic decision matrix from the weighted average.

$$D^* = D * \mathrm{W} \tag{18}$$

$$where\ d_{ij} = (a_{ij}, b_{ij}, c_{ij})$$

Step 5: Compute the negative and positive SVNN solutions: This is categorized as cost or benefit type. G_1 and G_2 re the benefit-and the cost-type criteria.

Doi: https://doi.org/10.54216/IJNS.240209
Received: December 25, 2023 Revised: February 09, 2024 Accepted: April 21, 2024

The positive solution corresponds to G_1.

$$\rho^+ = a_{\rho+w}(\beta_j), b_{\rho+w}(\beta_j), ac_{\rho+w}(\beta_j) \quad (19)$$

The negative solution corresponds to G_2.

$$\rho^- = (a_{\rho-w}(\beta_j), b_{\rho-w}\,(\beta_j), ac_{\rho-w}(\beta_j) \quad (20)$$

Where:

$$a_{\rho+w}(\beta_j) = \begin{cases} \max_i a_{\rho iw}(\beta_j), si\ j \epsilon G_1 \\ \min_i a_{\rho iw}(\beta_j), si\ j \epsilon G_2, \end{cases} \quad a_{\rho-w}(\beta_j) = \begin{cases} \min_i a_{\rho iw}(\beta_j), si\ j \epsilon G_1 \\ \max_i a_{\rho iw}(\beta_j), si\ j \epsilon G_2, \end{cases}$$

$$b_{\rho+w}(\beta_j) = \begin{cases} \max_i b_{\rho iw}(\beta_j), si\ j \epsilon G_1 \\ \min_i b_{\rho iw}(\beta_j), si\ j \epsilon G_2, \end{cases} \quad b_{\rho-w}(\beta_j) = \begin{cases} \min_i b_{\rho iw}(\beta_j), si\ j \epsilon G_1 \\ \max_i b_{\rho iw}(\beta_j), si\ j \epsilon G_2, \end{cases}$$

$$c_{\rho+w}(\beta_j) = \begin{cases} \max_i c_{\rho iw}(\beta_j), si\ j \epsilon G_1 \\ \min_i c_{\rho iw}(\beta_j), si\ j \epsilon G_2, \end{cases} \quad c_{\rho-w}(\beta_j) = \begin{cases} \min_i c_{\rho iw}(\beta_j), si\ j \epsilon G_1 \\ \max_i c_{\rho iw}(\beta_j), si\ j \epsilon G_2, \end{cases}$$

Step 6: Compute the distances to the negative and positive SVNN solutions:

$$d_i^+ = (\frac{1}{3}\sum_{j=1}^{n}\{(a_{ij} - a_j^+)^2 + (b_{ij} - b_j^+)^2 + (c_{ij} - c_j^+)^2\})^{\frac{1}{2}} \quad (21)$$

$$d_i^- = (\frac{1}{3}\sum_{j=1}^{n}\{(a_{ij} - a_j^-)^2 + (b_{ij} - b_j^-)^2 + (c_{ij} - c_j^-)^2\})^{\overline{2}} \quad (22)$$

Step 7: Computation of Coefficient of Proximity (CP): The PC of entire alternative is computed by the positive and negative solutions.

$$\widetilde{\rho_J} = \frac{s^-}{s^+ + s^-} \quad (23)$$

Where $0 \leq . \widetilde{\rho_J} \leq 1$

Step 8: Define the alternative orders: They are ordered based on they $\widetilde{\rho_J}$. The alternative is ordered from highest to lowest, thus $\widetilde{\rho_J} \to 1$ is the optimum solution.

4. Performance Validation

The performance validation of the NTOPSIS-TCIE approach can be studied using TC image dataset [22]. The dataset comprises 80 samples under four classes as defined in Table 1. Fig. 3 represents the sample images.

Table 1: Details of dataset

Classes	No. of Samples
Typhoon	20
Strong Typhoon	20
Very Strong Typhoon	20
Violent Typhoon	20
Total Samples	80

Doi: https://doi.org/10.54216/IJNS.240209
Received: December 25, 2023 Revised: February 09, 2024 Accepted: April 21, 2024

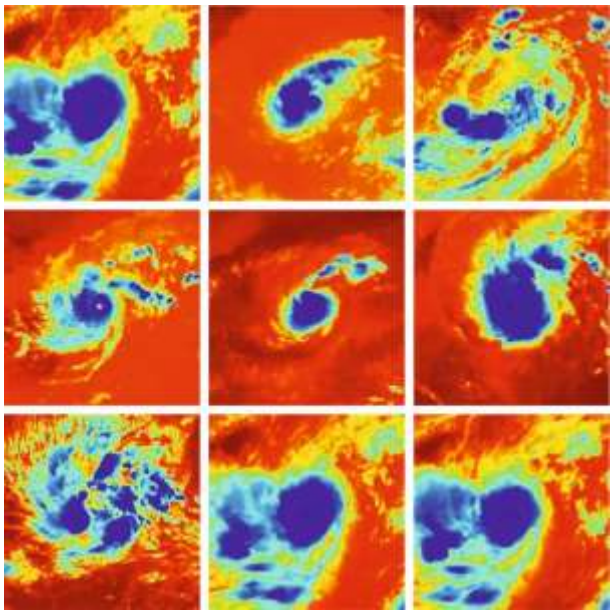

Figure 3: Sample images

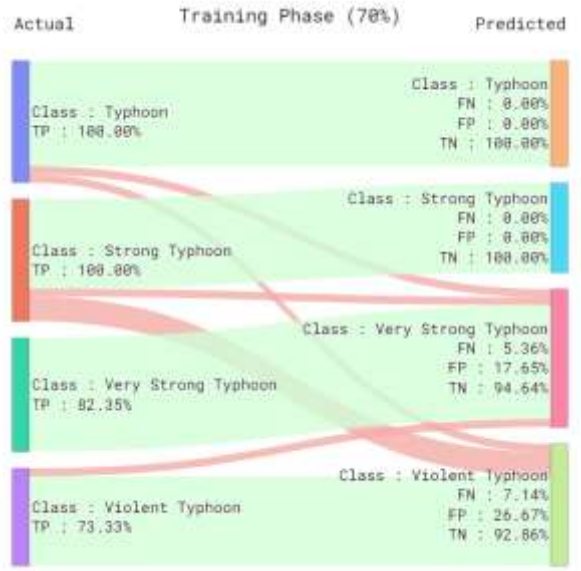

Figure 4: Confusion matrix of NTOPSIS-TCIE model under 70%TRAS

Fig. 4 establishes the confusion matrix attained by the NTOPSIS-TCIE algorithm under 70%TRAS. The outcomes implied that the NTOPSIS-TCIE methodology has accurate recognition and classification of all 4 classes accurately.

Doi: https://doi.org/10.54216/IJNS.240209
Received: December 25, 2023 Revised: February 09, 2024 Accepted: April 21, 2024

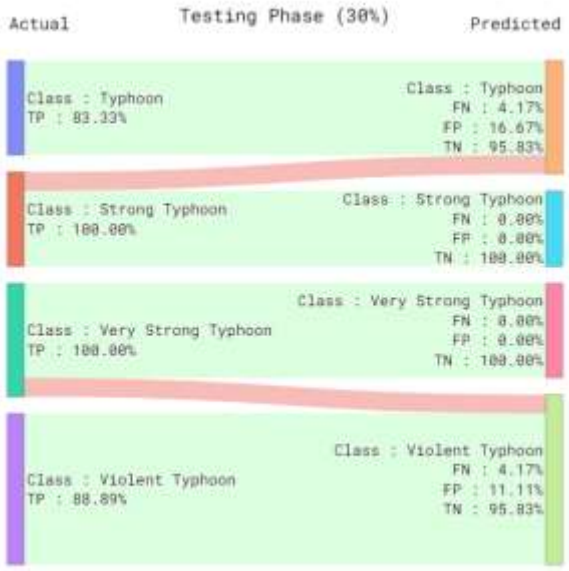

Figure 5: Confusion matrix of NTOPSIS-TCIE model under 30%TESS

Fig. 5 depicts the confusion matrix produced by the NTOPSIS-TCIE system under 30%TESS. The outcome stated that the NTOPSIS-TCIE approach has effectual recognition and classification of all 4 classes correctly.

The weather prediction outcome of the NTOPSIS-TCIE system is tested under 70%TRAS and 30%TESS in Table 2 and Fig. 6. The outcome implied that the NTOPSIS-TCIE method has resulted in enhanced performance. On 70%TRAS, the NTOPSIS-TCIE approach reaches average $accu_y$, $prec_n$, $sens_y$, $spec_y$, and F_{score} of 93.75%, 88.92%, 87.92%, 95.94%, and 87.32%, correspondingly. Likewise, on 30%TESS, the NTOPSIS-TCIE system obtains average $accu_y$, $prec_n$, $sens_y$, $spec_y$, and F_{score} of 95.83%, 93.06%, 90.83%, 97.12%, and 91.21%, correspondingly.

Table 2: Weather prediction outcome of NTOPSIS-TCIE technique under 70%TRAS and 30%TESS

Classes	$Accu_y$	$Prec_n$	$Sens_y$	$Spec_y$	F_{Score}
TRAS (70%)					
Typhoon	96.43	100.00	86.67	100.00	92.86
Strong Typhoon	92.86	100.00	73.33	100.00	84.62
Very Strong Typhoon	94.64	82.35	100.00	92.86	90.32
Violent Typhoon	91.07	73.33	91.67	90.91	81.48
Average	93.75	88.92	87.92	95.94	87.32
TESS (30%)					
Typhoon	95.83	83.33	100.00	94.74	90.91
Strong Typhoon	95.83	100.00	80.00	100.00	88.89
Very Strong Typhoon	95.83	100.00	83.33	100.00	90.91
Violent Typhoon	95.83	88.89	100.00	93.75	94.12

Doi: https://doi.org/10.54216/IJNS.240209
Received: December 25, 2023 Revised: February 09, 2024 Accepted: April 21, 2024

Average	95.83	93.06	90.83	97.12	91.21

Figure 6: Average of NTOPSIS-TCIE technique under 70%TRAS and 30%TESS

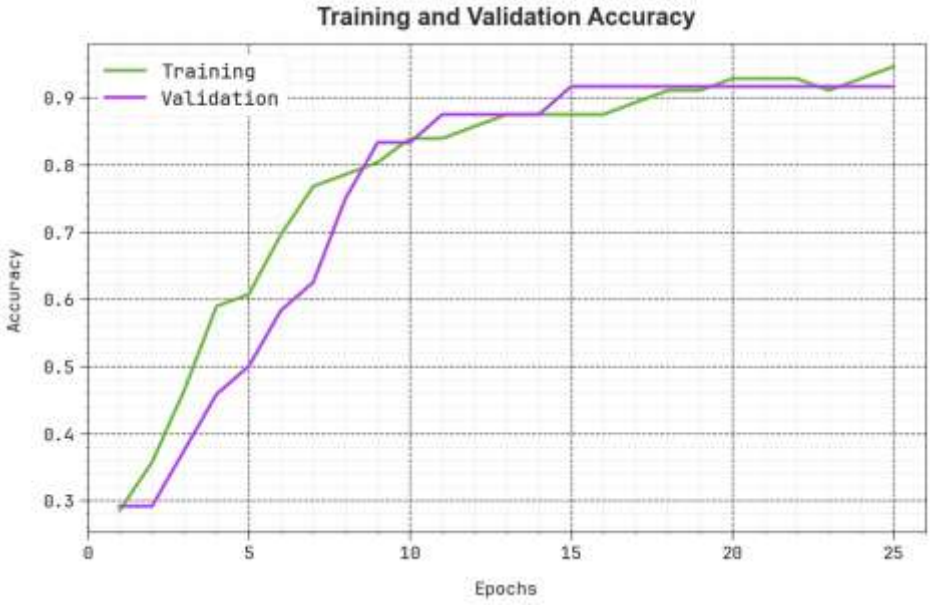

Figure 7: $Accu_y$ curve of the NTOPSIS-TCIE technique

The performance of the NTOPSIS-TCIE algorithm is clearly projected in Fig. 7 in the procedure of training accuracy (TRAA) and validation accuracy (VALA) curves. The outcome displays beneficial interpretation of the behaviour of NTOPSIS-TCIE algorithm under distinct epoch count, signifying its learning method and generalization abilities. Noticeably, the outcome infers a steady improvement in the TRAA and VALA with development in epochs. It makes sure the adaptive nature of the NTOPSIS-TCIE algorithm in the pattern recognition process on both data. The rising trend in VALA outlines the ability of the NTOPSIS-TCIE approach to adapt to the TRA data and excel in offering accurate classifiers on unnoticed data, demonstrating robust generalization proficiencies.

Fig. 8 determines a complete representation of the training loss (TRLA) and validation loss (VALL) results of the NTOPSIS-TCIE approach over distinct epochs. The progressive decrease in TRLA highlights the NTOPSIS-TCIE system optimizing the weights and diminishing the classification error on both data. The outcome signifies a clear

Doi: https://doi.org/10.54216/IJNS.240209
Received: December 25, 2023 Revised: February 09, 2024 Accepted: April 21, 2024

understanding of the NTOPSIS-TCIE approach's association with the TRA data, emphasizing its ability to capture patterns from both data. Remarkably, the NTOPSIS-TCIE model continually improves its parameters in decreasing the differences between the predictive and real TRA classes.

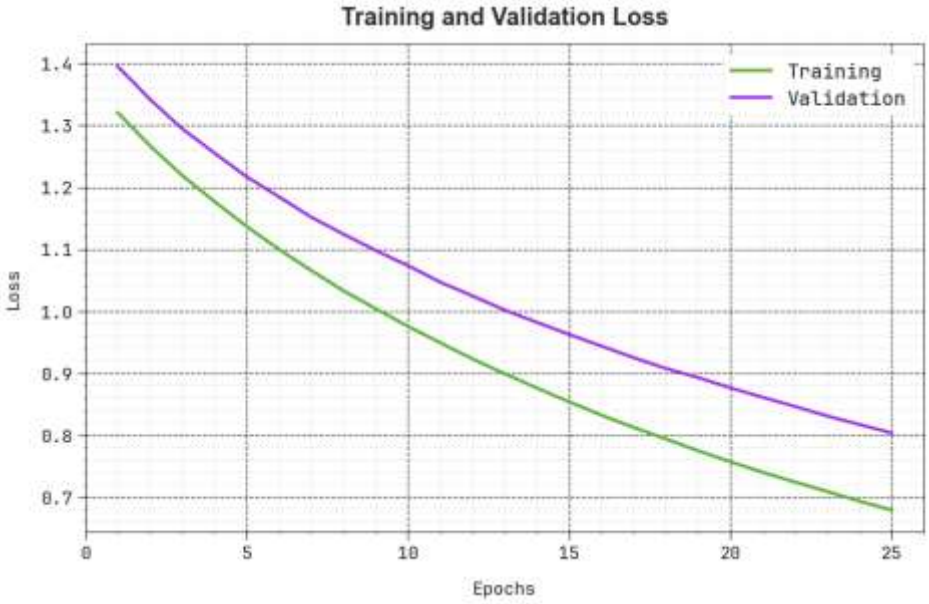

Figure 8: Loss curve of the NTOPSIS-TCIE technique

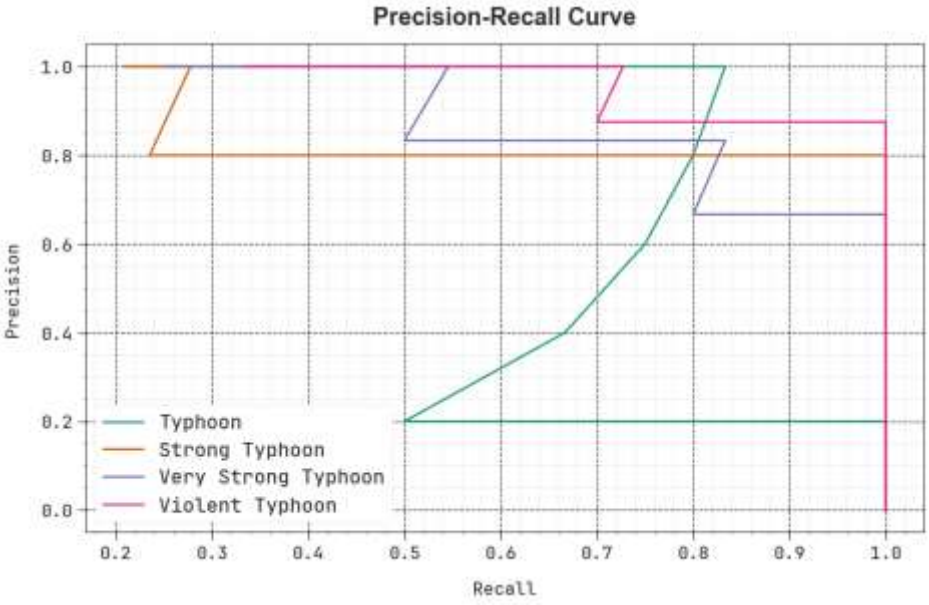

Figure 9: PR curve of the NTOPSIS-TCIE technique

Examining the precision-recall (PR) curve, as exhibited in Fig. 9, the outcome ensured that the NTOPSIS-TCIE algorithm progressively achieves greater value of PR under each class. It verifies the improved capabilities of the NTOPSIS-TCIE approach in the identification of different classes, demonstrating the ability of the detection classes.

Additionally, in Fig. 10, ROC curves created by the NTOPSIS-TCIE algorithm are depicted in the classification of various labels. It offers detailed understanding of the tradeoff among TPR and FRP under distinct detection threshold values and epoch counts. The outcome emphasized the improved classifier outcome of the NTOPSIS-TCIE methodology under all classes, outlining the efficiency in addressing several classifier issues.

Doi: https://doi.org/10.54216/IJNS.240209
Received: December 25, 2023 Revised: February 09, 2024 Accepted: April 21, 2024

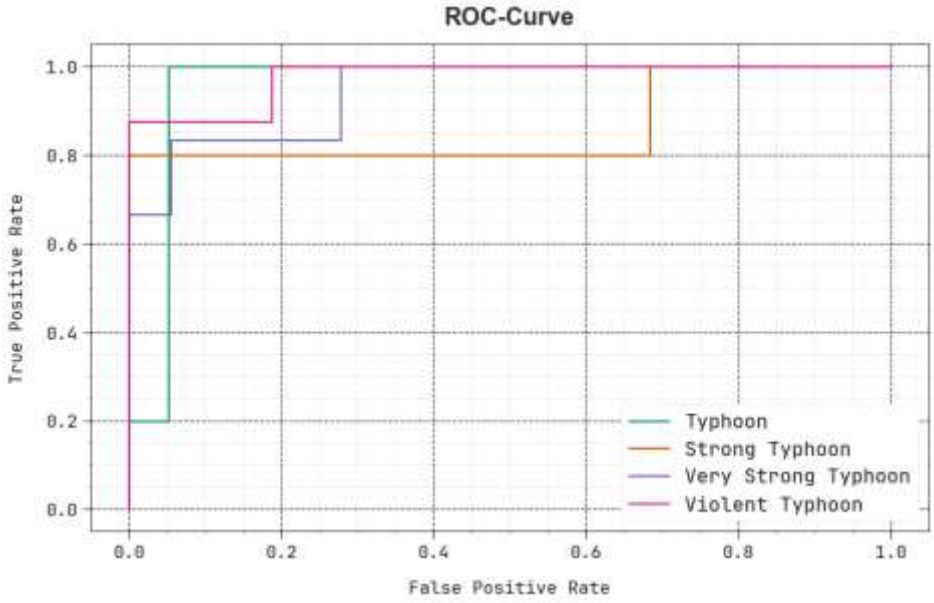

Figure 10: ROC curve of the NTOPSIS-TCIE technique

Table 3 and Fig. 11 display the overall comparison results of the NTOPSIS-TCIE technique with other models. The figure highlighted that the NTOPSIS-TCIE technique gains better performance. Based on $accu_y$, the NTOPSIS-TCIE approach offers enhanced $accu_y$ of 95.83% whereas the VGG16, VGG19, InceptionV3, GoogleNet, MLP, and DBN systems gain lower $accu_y$ of 94.23%, 94.12%, 91.63%, 90.85%, 90.31%, and 93.22%, correspondingly. Furthermore, based on $prec_n$, the NTOPSIS-TCIE technique offers increased $prec_n$ of 93.06% whereas the VGG16, VGG19, InceptionV3, GoogleNet, MLP, and DBN systems gain lesser $prec_n$ of 90.25%, 92.53%, 91.73%, 91.91%, 92.2%, and 90.8%, correspondingly. Eventually, based on F_{score}, the NTOPSIS-TCIE algorithm attains maximal F_{score} of 91.21% whereas the VGG16, VGG19, InceptionV3, GoogleNet, MLP, and DBN methodologies reach lesser F_{score} of 88.82%, 89.88%, 89.46%, 88.51%, 89.33%, and 90.77%, correspondingly.

Table 3: Comparative analysis of NTOPSIS-TCIE technique with other models

Classifiers	$Accu_y$	$Prec_n$	$Reca_l$	F_{Score}
NTOPSIS-TCIE	95.83	93.06	90.83	91.21
VGG16 Model	94.23	90.25	89.5	88.82
VGG19 Model	94.12	92.53	87.9	89.88
InceptionV3	91.63	91.73	85.47	89.46
GoogleNet	90.85	91.91	89.19	88.51
MLP Algorithm	90.31	92.2	88.97	89.33
DBN Model	93.22	90.8	86.73	90.77

Doi: https://doi.org/10.54216/IJNS.240209
Received: December 25, 2023 Revised: February 09, 2024 Accepted: April 21, 2024

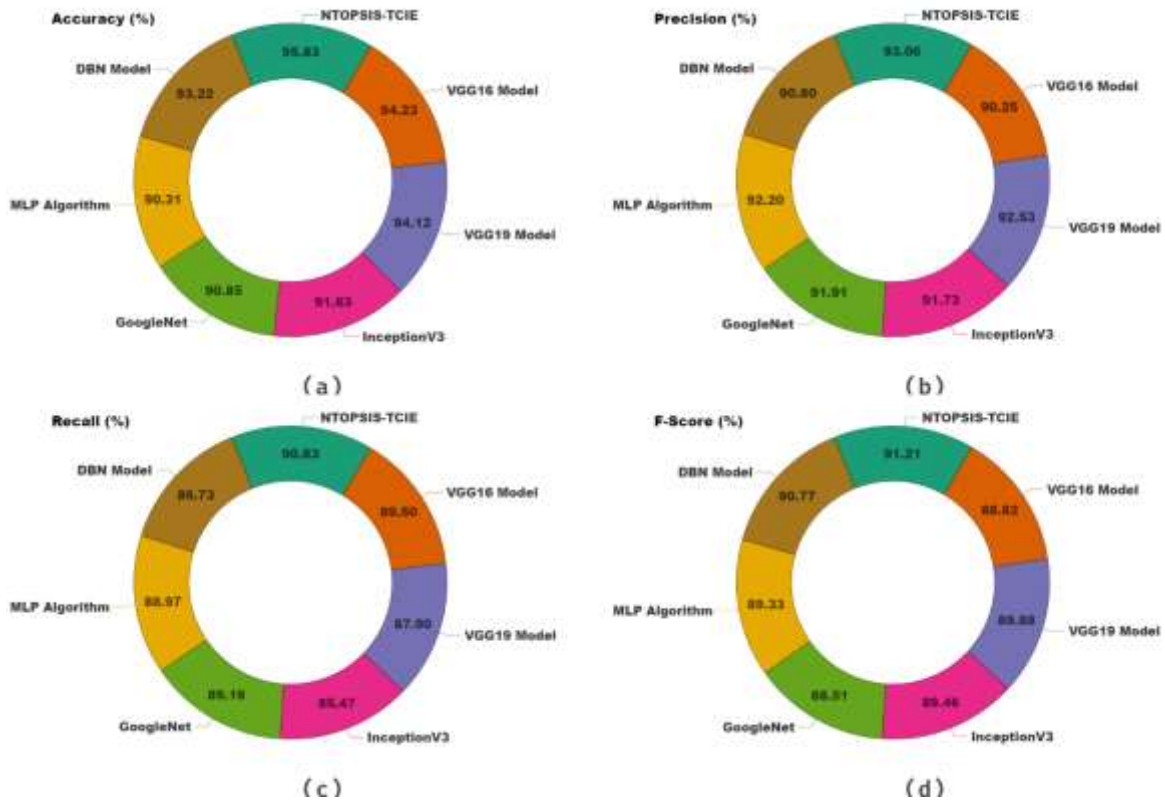

Figure 11: Comparative analysis of NTOPSIS-TCIE technique (a) $Accu_y$, (b) $Prec_n$, (c) $Reca_l$, and (d) F_{score}

5. Conclusion

In this study, we have presented a novel NTOPSIS-TCIE algorithm for weather prediction. The proposed NTOPSIS-TCIE method determines the intensities of the TC which in turn helps to forecast weather. It contains diverse kinds of processes involved as MF-based preprocessing, CNN-based feature extractor, HHO-based parameter tuning, and NTOPSIS-based TC prediction. At primary stage, the NTOPSIS-TCIE technique takes place MF approach is used to remove the noise in the images. In addition, the features are extracted using deep CNN model. To enhance the performance of the CNN model, HHO algorithm is applied. At last, the NTOPSIS approach can be deployed for the prediction of TC intensities. The performance of the NTOPSIS-TCIE technique can be studied using TC image dataset and the results signify its promising results over other models.

Funding: "This project is sponsored by Prince Sattam Bin Abdulaziz University (PSAU) as part of funding for its SDG Roadmap Research Funding Programme project number PSAU-2023 –SDG-89"

Conflicts of Interest: "The authors declare no conflict of interest."

References

[1] Meng, F., Yang, K., Yao, Y., Wang, Z. and Song, T., 2023. Tropical cyclone intensity probabilistic forecasting system based on deep learning. International Journal of Intelligent Systems, 2023.
[2] McNeely, T., Khokhlov, P., Dalmasso, N., Wood, K.M. and Lee, A.B., 2023. Structural forecasting for short-term tropical cyclone intensity guidance. Weather and Forecasting, 38(6), pp.985-998.
[3] Meng, F., Yao, Y., Wang, Z., Peng, S., Xu, D. and Song, T., 2023. Probabilistic forecasting of tropical cyclones intensity using machine learning model. Environmental Research Letters, 18(4), p.044042.
[4] Sun, J., Cai, M., Liu, G. and Zhang, D.L., 2024. A Comparative Study of Mathematical Models for the Tropical Cyclone Intensity–Size Relation. Ocean-Land-Atmosphere Research, 3, p.0035.
[5] Wang, C. and Li, X., 2023. Deep learning in extracting tropical cyclone intensity and wind radius information from satellite infrared images—A review. Atmospheric and Oceanic Science Letters, p.100373.
[6] Song, T., Yang, K., Li, X., Peng, S. and Meng, F., 2024. Probabilistic Estimation of Tropical Cyclone Intensity Based on Multi-Source Satellite Remote Sensing Images. Remote Sensing, 16(4), p.606.

Doi: https://doi.org/10.54216/IJNS.240209
Received: December 25, 2023 Revised: February 09, 2024 Accepted: April 21, 2024

[7] Wang, X., Jiang, H. and Guzman, O., 2024. Relating tropical cyclone intensification rate to precipitation and convective features in the inner core. Weather and Forecasting, 39(2), pp.351-368.
[8] Wang, W., Zhang, Z., Cangialosi, J.P., Brennan, M., Cowan, L., Clegg, P., Hosomi, T., Masaaki, I., Das, A.K., Mohapatra, M. and Sharma, M., 2023. A review of recent advances (2018-2021) on tropical cyclone intensity change from operational perspectives, Part 2: Forecasts by Operational Centers. Tropical Cyclone Research and Review.
[9] Fu, R., Hu, H., Wu, N., Liu, Z. and Jin, W., 2024. Spatiotemporal fusion convolutional neural network: tropical cyclone intensity estimation from multisource remote sensing images. Journal of Applied Remote Sensing, 18(1), pp.018501-018501.
[10] Wu, S.N., Soden, B.J. and Alaka Jr, G.J., 2023. The influence of radiation on the prediction of tropical cyclone intensification in a forecast model. Geophysical research letters, 50(2), p.e2022GL099442.
[11] Zhao, Z., Zhang, Z., Tang, P., Wang, X. and Cui, L., 2024. MT-GN: Multi-Task-Learning-Based Graph Residual Network for Tropical Cyclone Intensity Estimation. Remote Sensing, 16(2), p.215.
[12] Kim, J.H., Ham, Y.G., Kim, D., Li, T. and Ma, C., 2024. Improvement in forecasting short-term tropical cyclone intensity change and their rapid intensification using deep learning. Artificial Intelligence for the Earth Systems.
[13] Ma, Z., Yan, Y., Lin, J. and Ma, D., 2024. A Multi-Scale and Multi-Layer Feature Extraction Network with Dual Attention for Tropical Cyclone Intensity Estimation. IEEE Transactions on Geoscience and Remote Sensing.
[14] Kumar, J.S., Venkataraman, V., Meganathan, S. and Krithivasan, K., 2023. Tropical cyclone intensity and track prediction in the bay of Bengal using LSTM-CSO method. IEEE Access.
[15] Tian, W., Lai, L., Niu, X., Zhou, X., Zhang, Y. and Lim Kam Sian, K.T.C., 2023. Estimating tropical cyclone intensity using dynamic balance convolutional neural network from satellite imagery. Journal of Applied Remote Sensing, 17(2), pp.024513-024513.
[16] Ma, D., Wang, L., Fang, S. and Lin, J., 2023. Tropical cyclone intensity prediction by inter-and intra-pattern fusion based on multi-source data. Environmental Research Letters, 18(1), p.014020.
[17] Jiang, W., Hu, G., Wu, T., Liu, L., Kim, B., Xiao, Y. and Duan, Z., 2023. DMANet_KF: tropical cyclone intensity estimation based on deep learning and Kalman filter from multi-spectral infrared images. IEEE Journal of Selected Topics in Applied Earth Observations and Remote Sensing.
[18] Argilagos, M.R., Herrera, A.V. and Valdiviezo, W.V., 2022. Evaluation of nutritional education strategies in schools in ecuador using neutrosophic TOPSIS. International Journal of Neutrosophic Science, 18(3), pp.208-217.
[19] Adamu, M., Jiro, A.A., Abdul-Malik, U.T., Danlami, M. and Abdullahi, I.M., 2023. Enhanced Adaptive Threshold Median Filter For Medical Image Filtering. ATBU Journal of Science, Technology and Education, 11(2), pp.217-224.
[20] Chavan, R. and Pete, D., 2024. Automatic multi-disease classification on retinal images using multilevel glowworm swarm convolutional neural network. Journal of Engineering and Applied Science, 71(1), p.26.
[21] Jose, J. and Judith, J.E., 2024. Unveiling the IoT's dark corners: anomaly detection enhanced by ensemble modelling. Automatika, 65(2), pp.584-596.
[22] https://www.kaggle.com/datasets/sshubam/insat3d-infrared-raw-cyclone-images-20132021

Doi: https://doi.org/10.54216/IJNS.240209
Received: December 25, 2023 Revised: February 09, 2024 Accepted: April 21, 2024